

A Texas Instruments Application Report

MOSFET
fm tuner design 

MOSFET FM TUNER DESIGN

By
Richard Klein & Glen Coers

INTRODUCTION

Dual-gate MOSFETs in an FM tuner provide many advantages over bipolar, junction field-effect, and single-gate MOS field-effect transistors. RF amplification and mixing are aided by use of a low-feedback-capacitance transistor with low noise figure and large dynamic range. A second gate is available for either AGC or local oscillator injection. High, stable RF and conversion gains are easily obtained with inexpensive, commercially available coils and without need for neutralization. This report presents test data and design tips which can be used to design with the *3N201 dual-gate MOSFET at 100 MHz. The 3N201 is an N-channel, depletion mode, dual-gate, MOS transistor with integral back-to-back zener diodes between both gates and the source to eliminate the need for special precautionary handling procedures.

100-MHz RF AMPLIFIER

DC CONSIDERATIONS

Figure 1 shows some typical 3N201 device data. It is noted in Figure 1c that for the highest Gate-1-to-drain transconductance, Gate-1-to-source (V_{G1S}) voltage should be 0.5 volts. Figure 1e indicates nearly flat transconductance for Gate-2-to-source voltage (V_{G2S}) of 4 volts and above. (A resistance should be placed in series with Gate 2 to limit excessive gate zener current caused by accidental application of V_{G2S} voltages above the typical internal zener voltage of ± 12 volts.) To insure that the device is operated within its rated 450 mW, V_{G1S} should not exceed 0 volts with $V_{G2S} = 4$ volts and a 15-volt supply voltage. Operation of the device at I_{DSS} or $V_{G2S} = 4$ volts, $V_{G1S} = 0$ volts, $V_{DS} = 15$ volts, and $T_A = 25^\circ\text{C}$, will be discussed later.

Biasing the MOSFET at I_{DSS} may pose a power supply regulation problem. From Figure 1g, a unit-to-unit total spread of from 5 mA to 30 mA can be expected. This high current can be the cause of some troublesome ground loops and unwanted oscillator pulling with AGC action. A

suitable solution is the use of self-bias. Superimposed onto Figure 1g is a load line drawn to represent a 270-ohm source resistor and a 1.3-volt Gate-1-to-ground voltage. The obvious purpose of this combination is to reduce the steady-state bias current variation from 25 mA to 5 mA and to bias the typical I_{DSS} device at $1/2 I_{DSS}$.

GAIN AND STABILITY CONSIDERATIONS

The typical 3N201 100-MHz parameters are shown in Figures 1a through 1c. The reverse transfer admittance is too small to measure on the General Radio admittance bridge. Instead, a Boonton capacitance bridge was used to measure the 1-MHz reverse transfer capacitance, C_{RSS} . Further inspection of this data reveals that at 100 MHz the input and output conductances are too small to measure accurately. This makes an accurate design on paper very difficult, if not impossible, to prepare. Some insight can, however, be acquired on the problem of gain and stability by making the following assumptions (see Figures 2 and 3):

- 1) $Y_{RS} = j\omega (C_{RSS} + \text{stray cap.}) = 0.022 \text{ mmho}$
- 2) $\text{Re}(y_{is}) \ll G_s'$ (source conductance)
- 3) $\text{Re}(y_{os}) \ll G_L'$ (load conductance)
- 4) $G_s' = 1 \text{ mmho}$
- 5) $|Y_{fs}| = 12 \text{ mmho}$

Here it is assumed that the input conductance of the device is $\text{Re}(y_{is})$ and the output conductance is $\text{Re}(y_{os})$ as in the case of no feedback, Y_{RS} . A source conductance of 1 mmho was chosen to offer the best device noise figure, voltage gain from the antenna, and some mismatch to reduce skewing with AGC action. Tests have shown the device noise performance to be excellent for R_s' ranging from 1 k Ω to 2 k Ω . Care must be taken to shield the input circuitry from the output circuitry.

A figure of merit which can be used to estimate stability is defined by Stern¹:

$$K = \frac{2(g_{11} + G_s)(g_{22} + G_L)}{|Y_{12} Y_{21}| + \text{Re}(Y_{12} Y_{21})} \quad (1)$$

*3N201 is a special device fabricated by Texas Instruments Incorporated, Dallas, Texas.

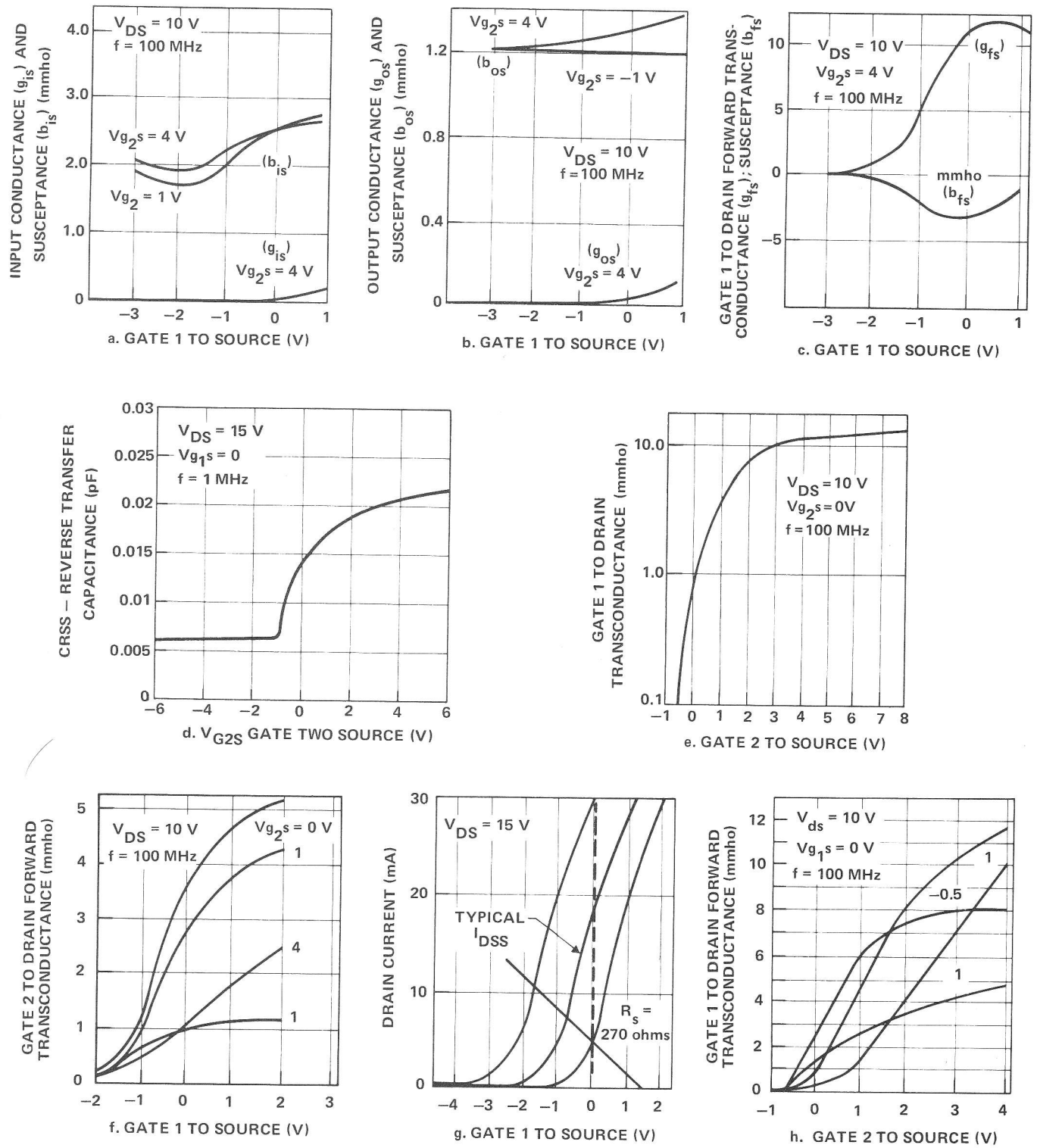


FIGURE 1. Device Data

where

K = stability factor;

$$R_L' = I/G_L';$$

$$R_S' = I/G_S'$$

Solving for R_L'

$$R_L' = \frac{2}{K R_S' [Y_{12} Y_{21}] + \text{Re}(Y_{12} Y_{21})} \quad (2)$$

For $K = 2$, $R_L' = 4.8 \text{ k}\Omega$, and from this the voltage gain is calculated to be

$$AV = |Y_{fs}| R_L' = 57.5 \quad (3)$$

$$LVG^* = 35.2 \text{ dB}$$

In reality this gain gave objectionable skewing in the test fixture. A more acceptable load was experimentally determined to be $2 \text{ k}\Omega$. Therefore $LVG = 27.6 \text{ dB}$.

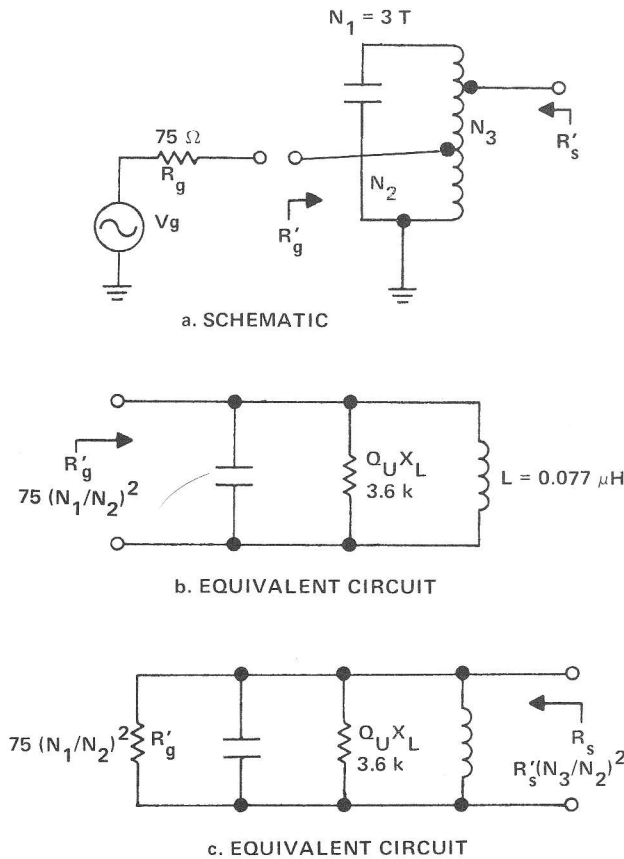


FIGURE 2. Input Coil

INPUT-COIL CONSIDERATIONS

The design of the input coil can proceed with the following assumptions (see Figure 2):

- 1) Loaded $Q < 40$
- 2) $VSWR = R_g'/R_g < 2:1$
- 3) $QU = 75$
- 4) $X_L = 48 \text{ ohms}$ ($0.077 \mu\text{H}$)
- 5) Device input resistance neglected.

An inductance of $0.077 \mu\text{H}$ was chosen, so that a standard tuning capacitor with a delta $C = 15 \text{ pF}$ would tune the 88-MHz-to-108-MHz FM band.² Unloaded Q 's of

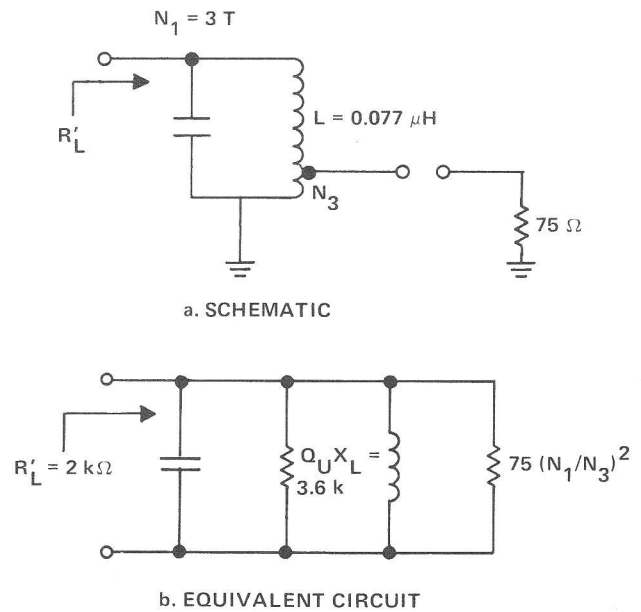


FIGURE 3. Output Coil

75 and 140 are easily obtained by proper choice of ferrite tuning slug.

The only resistance to be transformed down to match the 75-ohm antenna impedance is the coil loss QUX_L , with reference to Figure 2b,

$$(N_1/N_2)^2 = QU X_L / 75 = 48 \quad (4)$$

$$N_2 = 0.434 \text{ turns}$$

$$N_1 = 3 \text{ turns}$$

With reference to Figure 2c,

$$R_s = \frac{R_g' QU X_L}{R_g' + QU X_L} = 1.8 \text{ K} \quad (5)$$

$$N_3 = N_1 (R_s'/R_s)^{1/2} = 2.24 \quad (6)$$

$$Q_L = R_s / X_L = 37.5 \quad (7)$$

The coil loss, which directly contributes to noise figure, is the loaded to unloaded Q ratio.² For this case, $Q_L/Q_U = 0.5$ (6 dB). This is a significant degradation of noise performance. If the computations are performed again with a $VSWR = 2:1$ or $R_g' = 150 \text{ ohms}$ and an unloaded $Q = 140$, the new $Q_L = 36.3$ and $Q_L/Q_U = 0.26$ (-2.6 dB). The key here is relaxation of the allowable $VSWR$.

The input voltage gain for the first calculation is computed simply as

$$LVG = 20 \log_{10} (N_3/N_2) = 14.2 \text{ dB} \quad (8)$$

*LVG (log voltage gain) is used here to distinguish between voltage and power gain.

OUTPUT-COIL CONSIDERATIONS

Design of the output coil can proceed by making the following assumptions (see Figure 3a):

- 1) $40 < Q_L < 60$
- 2) $Q_U = 75$
- 3) $X_L = 48 \text{ ohms}$
- 4) Device output resistance neglected.

From Figure 3b solving for an $R_L' = 2 \text{ k}\Omega$

$$R_L' = 75 (N_1/N_3)^2$$

$$Q_U X_L / [75 (N_1/N_3)^2 + Q_U X_L] \quad (9)$$

$$N_3 = 0.387 \text{ turns}$$

$$V_g = (N_3/N_1) = 1/8 \text{ (LVG)} = (-17.8 \text{ dB}) \quad (10)$$

$$Q_L = R_L' / X_L = 41.5 \quad (11)$$

The total gain can now be calculated as

$$\text{Gain} = \text{input} + \text{device} + \text{output}$$

$$\text{Gain} = 11.8 + 27.6 + (-17.8) = 21.6 \text{ dB} \quad (12)$$

Note that this is power gain because both input and output impedances are the same.

With an input and output loaded $Q = 40$, the image frequency (100 MHz + 21.4 MHz) will be better than 50 dB down, a standard requirement of most radio manufacturers.³

CIRCUIT EVALUATION

This design was used as a guide to construct a test fixture. Tests were made to explore the gain characteristic, detuning of 100-MHz reference frequency, and 3-dB bandwidth changes with AGC action, as well as third-order intermodulation degradation.⁴ Three circuit configurations were used (Figures 4, 5, and 6). The circuit used to take the data shown in Figures 7a through 7c was biased at $I_d = 1/2 I_{DSS}$ and used fixed bias on Gate 1 while AGC was applied to Gate 2 only. The circuit of Figures 8a through 8d was biased at $I_d = 1/2 I_{DSS}$ and slaved Gate 1 to Gate 2 so that Gate 1 would come down with Gate 2. The circuit of Figures 9a through 9d was biased at I_{DSS} with AGC voltage applied to Gate 2. Some points of interest are:

- 1) 2 dB more gain when biased at I_{DSS}
- 2) Biasing $I_d = I_{DSS}$ results in a 2:1 increase in frequency shift (Figures 7b and 9b), an erratic bandwidth change (Figure 9c), and a slight worsening of the intermodulation figure (Figure 9d) with AGC over the Gate 1 fixed bias condition (Figure 7c).
- 3) Slaving Gate 1 reduces the low-attenuation frequency shift of some devices with AGC; increases gain-reduction slope, and increases the

intermodulation figure of merit of devices beyond 40 dB of attenuation.

- 4) The best intermodulation figure was obtained at $I_d = 1/2 I_{DSS}$ and fixed bias on Gate 1 (Figure 7c).
- 5) Devices with steepest gain-reduction slopes tend to have the worst intermodulation figures.
- 6) The device tended to be more stable with less skewing when biased at $1/2 I_{DSS}$.

THE MIXER

A test fixture was constructed to measure the conversion gain and $f_o + 1/2$ IF distortion for a variety of bias conditions. Data are presented for both Gate 1 and Gate 2 local oscillator injection. The mixer was similarly constructed to the RF amplifier, except that a 10.7-MHz series trap was used at Gate 1, and a tuned load of approximately 5 k Ω at 10.7 MHz.

Figures 10a and 10b contain (for the bias point) conversion power gain versus oscillator injection and $f_o + 1/2$ IF distortion (dB) versus oscillator injection for the case of Gate 1 injection. It is interesting to note the flatness of these curves above 600 mV rms oscillator injection. A conversion gain of 20 dB was typical, as was an $f_o + 1/2$ IF spurious rejection of 55 dB. The spurious test was made with no gate selectivity for a worst-case analysis. The low pinch-off devices (-2 V at $20 \mu\text{A } I_d$) gave a gain of typically 22 dB; high pinch-off devices (-5 V at $20 \mu\text{A } I_d$) gave gains of typically 18 dB.

Figures 10c and 10d show that, by injecting the local oscillator into Gate 2 an average conversion gain of 14 dB was observed, and 65 dB $I_o + 1/2$ IF spurious rejection. With the local oscillator set to 3 volts rms, spurious rejection was 68 dB. This form of injection eliminates, for all practical purposes, the interaction often observed between RF and oscillator circuits during alignment.

A complete tuner was built with injection at Gate 1 (Figure 11). Performance specifications are as follows:

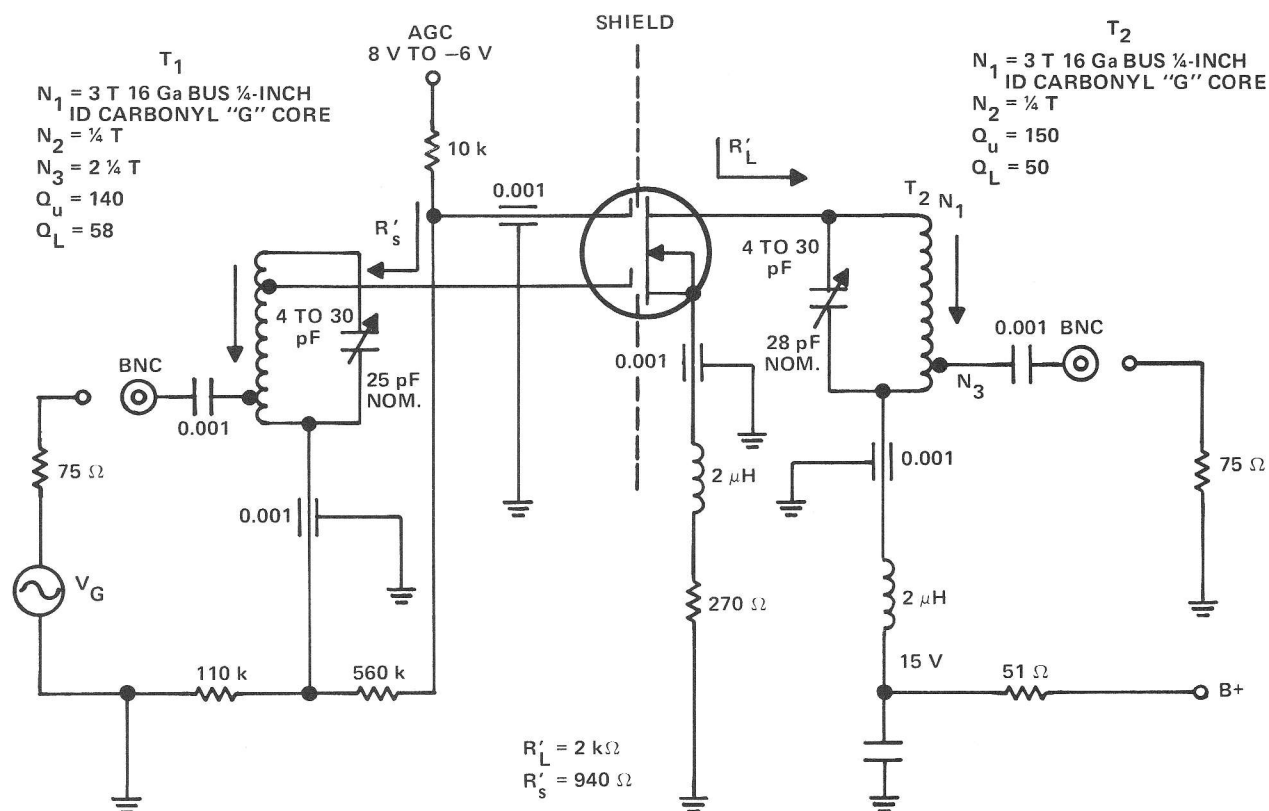
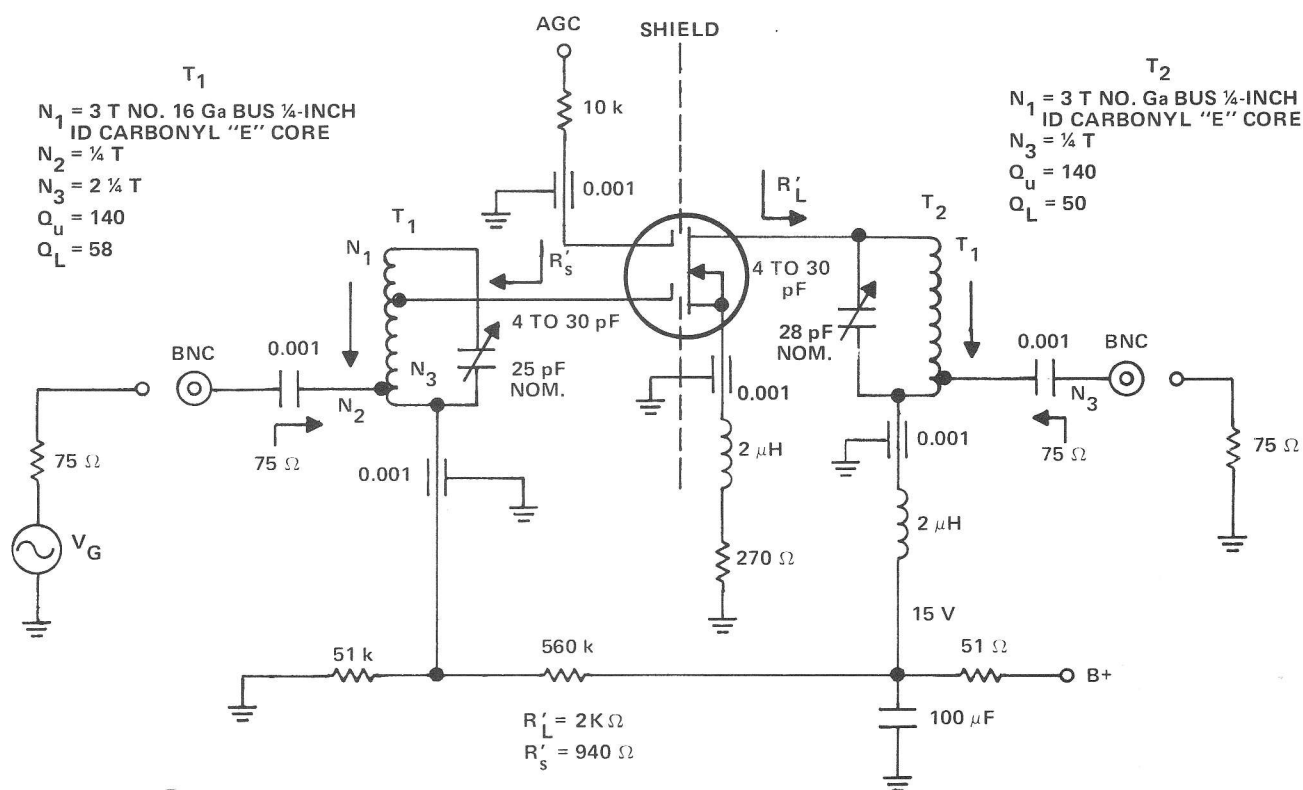
| | |
|--------------------|--------------------|
| Power gain | 40 dB |
| 3-dB limiting | $0.9 \mu\text{V}$ |
| 30-dB quieting | $*1.5 \mu\text{V}$ |
| Image rejection | 50 dB |
| $f_o + 1/2$ IF | 80 dB |
| All other spurious | > 100 dB |
| VSWR | 1.2:1 |

Measurements taken with a conventional four-stage IF amplifier. Test frequency, 100 MHz \pm 75 kHz.

CONCLUSIONS

The dual-gate MOSFET is well suited to FM tuner service as an RF amplifier and as a mixer. As an amplifier it provides high gain, low noise, and a large AGC range

* $0.7 \mu\text{V}$ with VSWR = 2:1



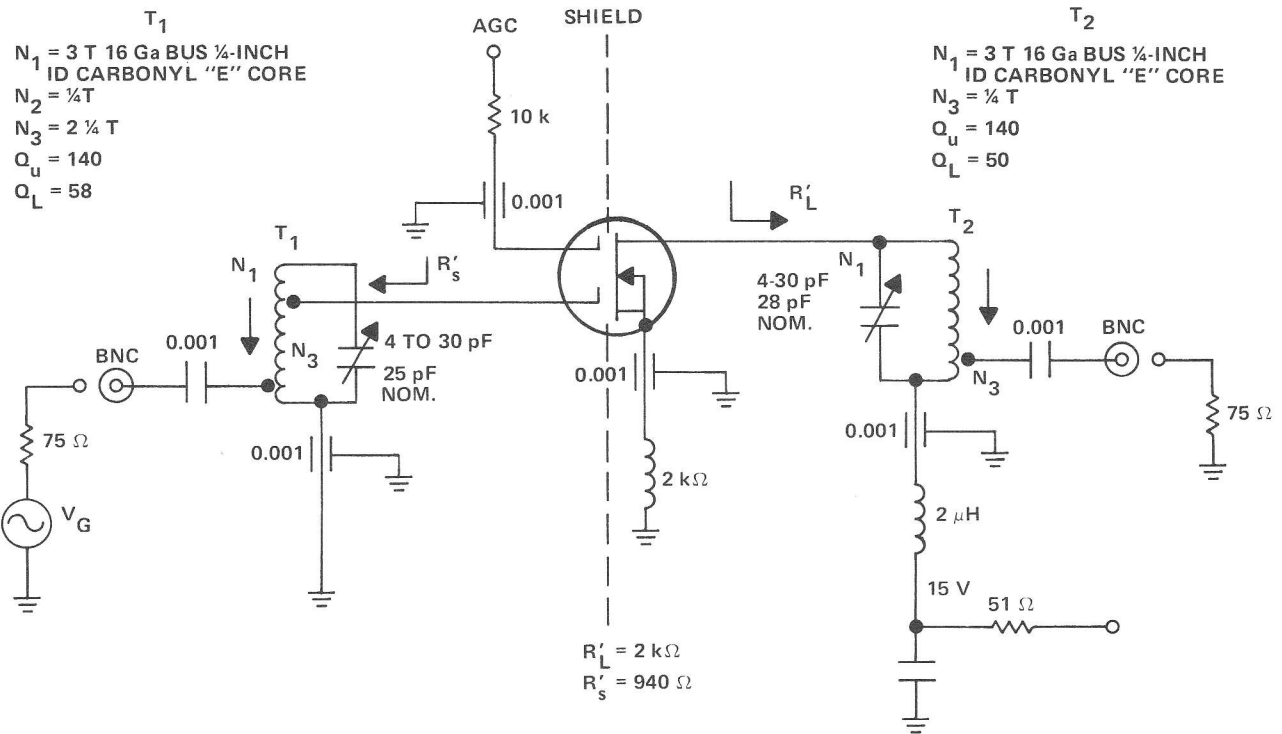


FIGURE 6. I_{DSS} Test Fixture

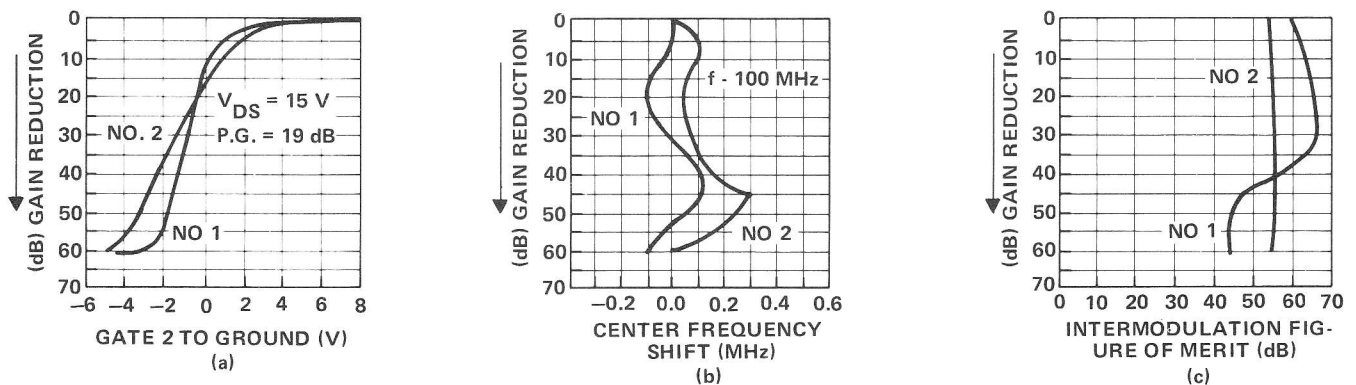


FIGURE 7. RF Performance Data with Gate 1 Fixed Biased (Schematic, Figure 4)

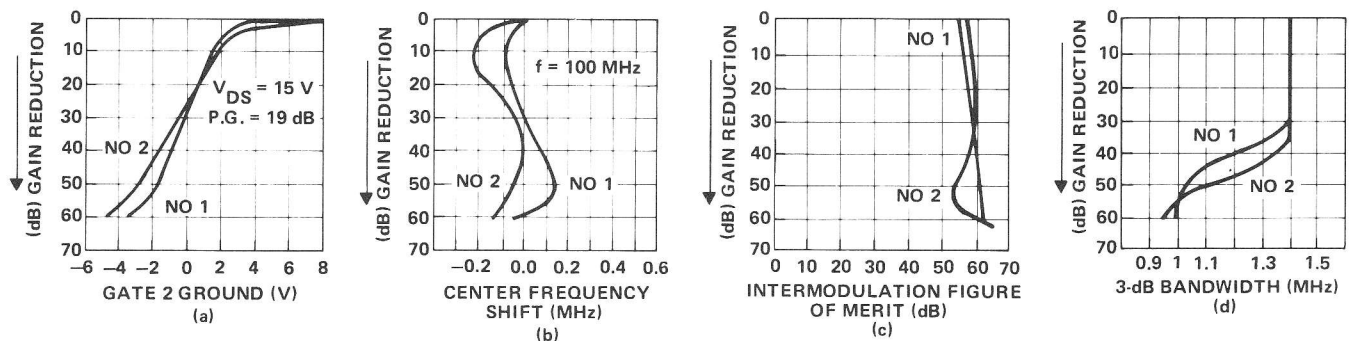


FIGURE 8. RF Performance Data with Gate 1 Slaved to Gate 2 (Schematic, Figure 5)

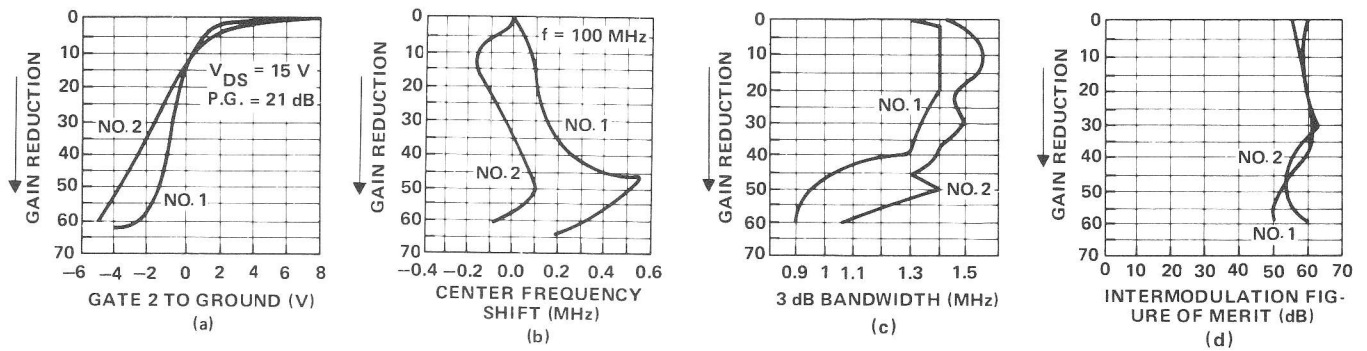


FIGURE 9. RF Performance Data Biased at I_{DSS} (Schematic, Figure 6)

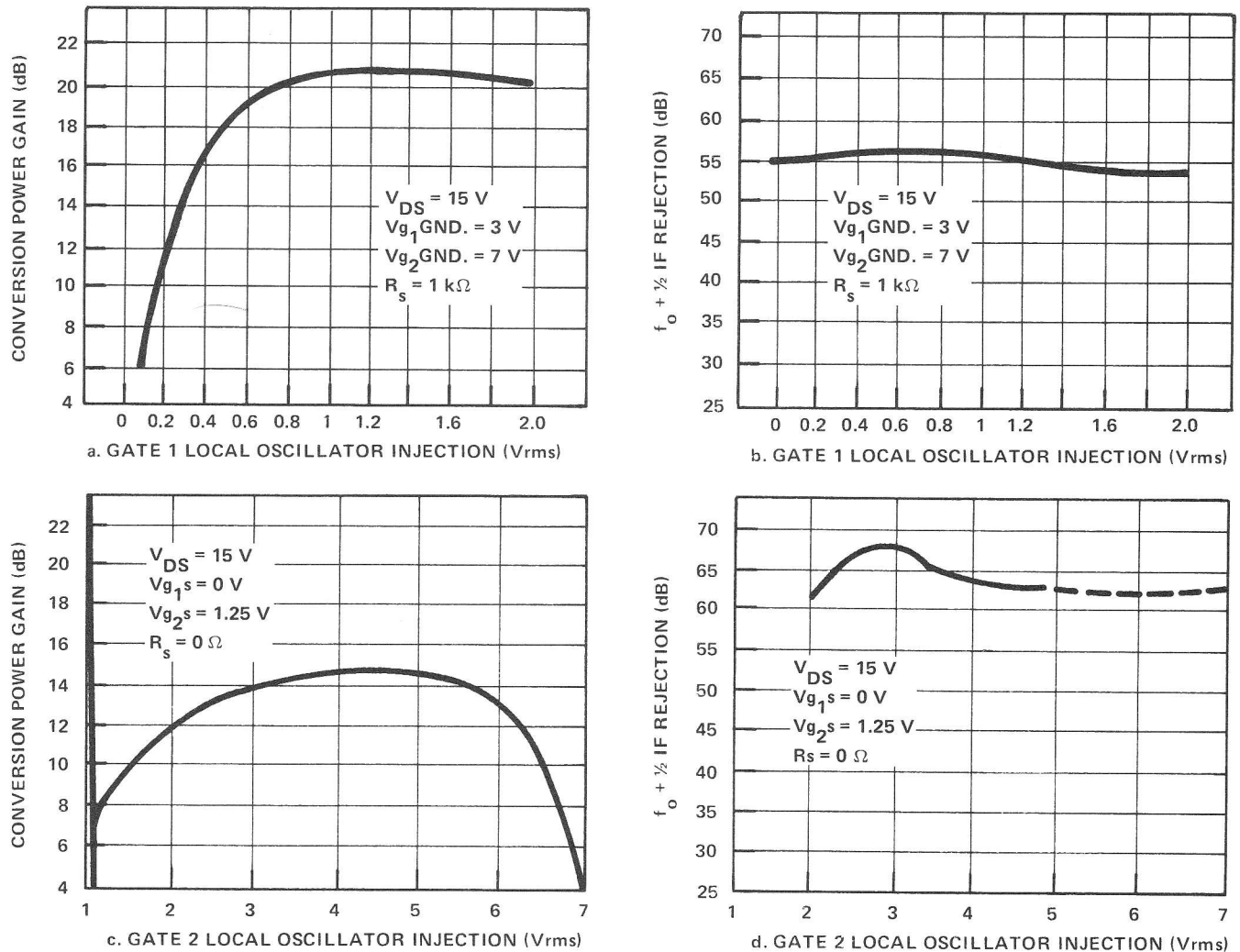


FIGURE 10. Mixer Performance Data (Schematic, Figure 11)

without overload. As a mixer the dual-gate MOSFET has large conversion gain and high spurious rejection. Gate 2 L.O. injection offers 10 dB better spurious rejection but requires three times the signal. Gate 2 local oscillator injection does have an average of 6 dB less gain than Gate 1, but the gain loss necessary to eliminate all signs of RF L.O. interaction could easily make up the difference.

REFERENCES

1. Texas Instruments Incorporated, *Solid-State Communications*, New York, McGraw-Hill Book Company (1966), pp. 64-65.
2. Texas Instruments Incorporated, *Circuit Design for AM/FM, and TV*, New York, McGraw-Hill Book Company (1967), p. 113.

TI worldwide sales offices

ALABAMA

Sahara Office Park Bldg., Suite 111
3313 Memorial Parkway, S.W.
Huntsville, Alabama 35801
205-881-4061

ARIZONA

United Bank Bldg., Suite 1702
3550 North Central Avenue
Phoenix, Arizona 85012
602-279-5531

CALIFORNIA

11222 South La Cienega,
Suite 360
Inglewood, California 90304
213-649-2710

753 North Pastoria Avenue
Sunnyvale, California 94086
408-732-1840

1505 East 17th St., Suite 201
Santa Ana, California 92701
714-547-6506

Balboa Towers Bldg., Suite 805
5252 Balboa Avenue
San Diego, California 92117
714-279-2622

COLORADO

2186 South Holly St., Suite 205
Denver, Colorado 80222
303-758-2151

CONNECTICUT

300 Amity Road
Woodbridge, Connecticut 06525
203-389-4521

FLORIDA

601 W. Oakland Park Blvd.
Fort Lauderdale, Florida 33311
305-566-3294

5400 Diplomat Circle
Diplomat Bldg., Suite 252
Orlando, Florida 32810
305-644-3535

300 Bldg. West, Suite 204
3151 Third Ave., North
St. Petersburg, Florida 33713
813-898-0807

ILLINOIS

1701 Lake Street, Suite 300
Glenview, Illinois 60025
312-729-5710
Effective November 1, 1971

INDIANA

8539 Encanto Way
Ft. Wayne, Indiana 46805
219-485-1959

MASSACHUSETTS

60 Hickory Drive
Waltham, Mass. 02154
617-890-7400

MICHIGAN

Central Park Plaza
26111 Evergreen, Suite 333
Southfield, Michigan 48075
313-352-5720

MINNESOTA

7615 Metro Blvd.
Suite 202, Analysis Inc., Bldg.
Edina, Minn. 55435
612-941-4384

NEW JERSEY

25 U.S. Highway #22
Springfield, New Jersey 07081
201-376-9400

NEW MEXICO

Suite 9, Marberry Plaza
6101 Marble Avenue, N.W.
Albuquerque, New Mexico 87110
505-265-8491

NEW YORK

P.O. Box 618, 112 Nanticoke Ave.
Endicott, New York 13760
607-785-9987

245 Newtown Road
Plainview, New York 11803
516-293-2560

167 Main Street
Fishkill, New York 12524
914-896-6793

7 Adler Drive
East Syracuse, New York 13057
315-463-9291

NORTH CAROLINA

4310 Starmount Dr.
Greensboro, N.C. 27410
919-299-9112

OHIO

23811 Chagrin Blvd., Suite 100
Cleveland, Ohio 44122
216-464-1192

Suite 205, Paul Welch Bldg.
3300 South Dixie Dr.
Dayton, Ohio 45439
513-298-7513

PENNSYLVANIA

275 Commerce Drive
Fort Washington, Pa. 19034
215-643-6450

TEXAS

MS366-P.O. Box 5012
Dallas, Texas 75222
214-238-6805

3939 Ann Arbor
Houston, Texas 77042
713-785-6906

WASHINGTON

5801 Sixth Ave. S.
Seattle, Washington 98108
206-762-4240

WASHINGTON, D.C.

1500 Wilson Blvd., Suite 1100 A.M. Bldg.
Arlington, Virginia 22209
703-525-0336

ARGENTINA

Texas Instruments Argentina S.A.I.C.F.

C.C. Box 2296-Correo Central
Buenos Aires, Argentina
744-1041

ASIA

Texas Instruments Asia Limited

5F Aoyama Tower Bldg.
24-15 Minami Aoyama Chome
Minato-ku, Tokyo 107, Japan
402-6171

Room 1502, Star House
Harbour Center, Kowloon
Hong Kong
K673139

Texas Instruments Taiwan Limited
P. O. Box 3999
Taipei, Chung Ho, Taiwan
923 904

AUSTRALIA

Texas Instruments Australia Ltd.

P.O. Box 63, 171-175 Philip Highway
Elizabeth, South Australia
55 29 14

Room 5, Rural Bank Bldg.
38 Railway Parade
Burwood N.S.W. Australia
74-1859

BRAZIL

Texas Instrumentos Electronicos
do Brasil Ltda.

Rua Cesario Alvim 770
Caixa Postal 30.103
Sao Paulo 6, Brasil
93-8278

CANADA

Texas Instruments Incorporated

2750 Pitfield Blvd.
St. Laurent 386
Quebec, Canada
514-332-3550

CANADA (Cont'd)

5F Caesar Avenue
Ottawa 12
Ontario, Canada
613-825-3716

280 Centre Str. East
Richmond Hill (Toronto)
Ontario, Canada
416-889-7373

DENMARK

Texas Instruments A/S

46D, Marielundvej
2730 Herlev, Denmark
91 74 00

FINLAND

Texas Instruments Finland OY

Fredrikinkatu 56, D 38
Helsinki 10, Finland
44 12 75

FRANCE

Texas Instruments France

Boite Postale 5
06 Villeneuve-Loubet, France
31 03 64

379 Av de la Liberation
92 Clamart, France
644 55 30

30-31 Quai Rambaud
69 Lyon, France
42 78 50

Ces des Fourches
Boulevard Frederic Chapplet
53 Laval, France
90 09 46

20, Avenue Honore Serres
31 Toulouse, France
62 82 85

GERMANY

Texas Instruments Deutschland GmbH

Haggerty Str. 1
8050 Freising, Germany
08161/7531

Arabellastrasse 4, Sternhaus/V
8000 Munich 81, Germany
0811/91 10 61-9

Lazarettstr. 19
4300 Essen, Germany
2141/20916

Krugerstrasse 24
1000 Berlin 49, Germany
0311/74 44 041

Westendstrasse 52
6000 Frankfurt a.M., Germany
0611/72 64 41

Am Mittelfelde 169
3000 Hannover, Germany
0511/86 10 16

Im Kaisemer 5
7000 Stuttgart 1, Germany
0711/22 38 20

ITALY

Texas Instruments Italia SpA

Casella Postale (P.O. Box) 156
02100 Rieti, Italy
43634

Viale Lunigiana 46
20125 Milano, Italy
688 31 41

Via Val di Chiana 56
50127 Firenze, Italy
512 36 10

Via Padre Smeria
00154 Roma, Italy
512 36 10

Via Barbaroux 2
10122 Torino, Italy
54 06 93

MEXICO

Texas Instruments de Mexico S.A.

Poniente 116 #489
Col. Industrial Vallejo
Mexico City, D.F., Mexico
567-92-00

NETHERLANDS

Texas Instruments Holland N.V.

Entrepot Gebouw-Kamer 223
P.O. Box 7603
Schiphol-Centrum
020-15 92 93

SWEDEN

Texas Instruments Sweden AB

S-104 40 Stockholm 14
Skeppargatan 26
67 98 35

UNITED KINGDOM

Texas Instruments Limited

Manton Lane
Bedford, England
67466

165 Bath Road
Slough, Buckinghamshire, England
Slough 33411

2259 Coventry Road
Sheldon, Birmingham 26, England
021-743-5293

24 Rutland Street
Edinburgh EH12AN, Scotland
031-229-1481

46 F. Nichols Road
Southampton, Hants, England
0703-27267

Mersey House
Heaton Mersey
Stockport, Cheshire, England
(061)432-0645